



HHS Public Access

Author manuscript

J Nutr Biochem. Author manuscript; available in PMC 2018 July 01.

Published in final edited form as:

J Nutr Biochem. 2017 July ; 45: 15–23. doi:10.1016/j.jnutbio.2017.02.022.

Trehalose supplementation reduces hepatic endoplasmic reticulum stress and inflammatory signaling in old mice

Michael J. Pagliassotti^{a,*}, Andrea L. Estrada^a, William M. Hudson^a, Yuren Wei^a, Dong Wang^a, Douglas R. Seals^b, Melanie L. Zigler^b, and Thomas J. LaRocca^b

^aDepartment of Food Science and Human Nutrition, Colorado State University, Fort Collins, CO, 80523-1571, USA

^bDepartment of Integrative Physiology, University of Colorado, Boulder, CO, 80309, USA

Abstract

The accumulation of damaged proteins can perturb cellular homeostasis and provoke aging and cellular damage. Quality control systems, such as the unfolded protein response (UPR), inflammatory signaling and protein degradation, mitigate the residence time of damaged proteins. In the present study, we have examined the UPR and inflammatory signaling in the liver of young (~6 mo.) and old (~28 mo.) mice (n=8/group), and the ability of trehalose, a compound linked to increased protein stability and autophagy, to counteract age-induced effects on these systems. When used, trehalose was provided for 4 wks in the drinking water immediately prior to sacrifice (n=7/group). Livers from old mice were characterized by activation of the UPR, increased inflammatory signaling and indices of liver injury. Trehalose treatment reduced the activation of the UPR and inflammatory signaling, and reduced liver injury. Reductions in proteins involved in autophagy and proteasome activity observed in old mice were restored following trehalose treatment. The autophagy marker, LC3B-II, was increased in old mice treated with trehalose. Metabolomics analyses demonstrated that reductions in hexosamine biosynthetic pathway metabolites and nicotinamide in old mice were restored following trehalose treatment. Trehalose appears to be an effective intervention to reduce age-associated liver injury and mitigate the need for activation of quality control systems that respond to disruption of proteostasis.

Keywords

Aging; inflammation; unfolded protein response; liver; hexosamine biosynthetic pathway; proteostasis

*Correspondence: Michael J. Pagliassotti, Department of Food Science and Human Nutrition, Colorado State University, Fort Collins, CO 80523-1571; Tel.: 970-491-1390, Fax: 970-491-3875; michael.pagliassotti@colostate.edu.

Author Contributions

MJP, ALE, DRS, MLZ, TJL contributed to the conception and design of experiments, analysis and interpretation of data. ALE, WMH, YW and DW contributed to the analysis and interpretation of data. MJP wrote the manuscript. ALE, DRS, MLZ, TJL edited the manuscript. All authors provided final approval of the submitted manuscript.

Publisher's Disclaimer: This is a PDF file of an unedited manuscript that has been accepted for publication. As a service to our customers we are providing this early version of the manuscript. The manuscript will undergo copyediting, typesetting, and review of the resulting proof before it is published in its final citable form. Please note that during the production process errors may be discovered which could affect the content, and all legal disclaimers that apply to the journal pertain.

1. Introduction

Trehalose is a non-reducing disaccharide composed of two glucose molecules connected by an alpha, alpha-1,1 linkage [1]. Trehalose displays many remarkable qualities including the ability to stabilize proteins and activate autophagy [1–3]. For example, oral administration of trehalose reduced polyglutamine aggregates in the cerebrum and liver in a transgenic mouse model of Huntington disease via mechanisms that involved stabilization of partially unfolded polyglutamine-containing protein [2]. Similarly, oral administration of trehalose ameliorated dopaminergic and tau pathology in parkin deleted/tau overexpressing mice [3]. More recently, trehalose induced hepatocyte autophagy and mitigated hepatocyte steatosis in response to a high fructose diet [4]. Results such as these suggest that trehalose may be a relevant therapeutic agent in chronic disease and age-associated pathologies linked to impairments in protein homeostasis (proteostasis).

Impairments in proteostasis are a common feature of aging, and collapse of proteostasis has been postulated as a fundamental mechanism leading to protein and cellular damage not only in aging, but also in metabolic diseases, such as obesity and non-alcoholic fatty liver disease [5, 6]. Proteostasis is monitored and maintained by complex quality control systems that include the cytosolic heat shock response, mitochondrial unfolded protein response and endoplasmic reticulum unfolded protein response (ER UPR) [6]. The ER UPR interacts with insulin signaling and inflammatory signaling pathways that are also characterized by impaired regulation in aging and metabolic diseases [7, 8]. Therefore, it has been postulated that the ER UPR can initiate inflammation, and the coupling of the ER UPR and inflammatory signaling may be a fundamental component of age- and disease-associated cellular stress and inflammation [7, 9].

Older age has been associated with several changes in the liver and hepatic sinusoid including thickening of the liver sinusoidal endothelial cell, deposition of perisinusoidal basal lamina and collagen, increased numbers of activated Kupffer cells, reductions in protein chaperone function and increased stress-induced activation of the ER UPR, and increased inflammation [10–14]. Recent studies have suggested that genetic and pharmacologic approaches that reduce inflammation or enhance protein degradation improve life span and age-associated liver damage [13, 14]. Therefore, one aim of this study was to examine the ER UPR and inflammatory signaling in the liver of old and young mice, and to determine whether trehalose can mitigate age-associated changes in these signaling pathways.

It has been suggested that the metabolism of trehalose is similar to that of glucose, given that trehalose is thought to be rapidly hydrolysed to glucose by the enzyme trehalase. Trehalase has been found in humans and most animals at the brush border of the intestinal mucosa, as well as in the kidney, liver and circulation [15–17]. Thus, trehalose metabolism does not appear to be consistent with its ability to improve proteostasis or activate degradative pathways. Therefore, the second aim of this study was to examine the metabolite profile in the liver of old and young mice in the absence and presence of trehalose supplementation.

2. Materials and Methods

2.1 Animals

Experiments were performed on frozen livers from male C57BL/6 mice, an established model of aging [18, 19]. These animals were obtained from the National Institute on Aging rodent colony and housed in an animal care facility at the University of Colorado at Boulder on a 12:12 h light-dark cycle. The mice were group housed and fed ad libitum until time of sacrifice. The mice were divided into four groups: young control, young + trehalose, old control, and old + trehalose. The young mice were 5–6 months old at the time of sacrifice and the old were 27–28 months (n=8/group). The treatment groups received 2% trehalose in their drinking water for four weeks leading up to sacrifice (n=7/group). Mice were anaesthetized using isoflurane and killed by exsanguination via cardiac puncture. All procedures conformed to the *Guide for the Care and Use of Laboratory Animals* (NIH publication no. 85–23, revised 2011) and were approved by the University of Colorado at Boulder Animal Care and Use Committee [18].

2.2 Plasma Analyses

Plasma glucose and triglycerides were determined enzymatically using reagent kits (Sigma, St. Louis, MO). Plasma aspartate aminotransferase and alanine aminotransferase were analyzed using kits (Abcam, Cambridge, MA). Plasma IL-1 β and IL-6 were measured by bead assay (eBioscience, San Diego, CA) and IL-18 by ELISA (RayBiotech, Norcross, GA).

2.3 Liver Triglycerides

Liver lipid was extracted using the procedure of Bligh and Dyer [20]. Triglyceride concentration was determined using a kit (Sigma).

2.4 Liver Caspase-1 and Proteasome Activity

Liver caspase-1 and proteasome activity were determined fluorometrically (BioVision, Milpitas, CA). The caspase-1/ICE fluorometric assay kit is based on detection of cleavage of substrate YVAD-AFC (AFC: 7-amino-4-trifluoromethyl coumarin). The proteasome activity assay takes advantage of the chymotrypsin-like activity of the 20S proteasome assembly by utilizing an AMC-tagged peptide substrate which releases free, highly fluorescent AMC in the presence of proteolytic activity. Proteasome activity was differentiated from other protease activity using the proteasome inhibitor MG-132, which suppresses all proteolytic activity due to proteasomes.

2.5 Polysome Fractionation

Liver tissue was pulverized in liquid nitrogen and lysed with NP40-lysis buffer (10 mM Tris-HCL at pH 8.0, 150 mM NaCl, 5 mM MgCl₂, 1% Nonidet-P40, 40 mM dithiothreitol, 500 U/ml RNasin and 1% (w/v) deoxycholate) [21]. Nuclei were removed via centrifugation (12,000g, 10 sec, 4°C) and the supernatant was supplemented with 500 μ l of 2X extraction buffer (0.2 M Tris-HCL at pH 7.5, 0.3 M NaCl), 150 μ g/ml cycloheximide, 650 μ g/ml heparin, and 10 mM phenyl-methyl-sulfonyl fluoride, and centrifuged (12,000g, 5 min, 4°C) to remove mitochondria and membrane debris [21]. The supernatant was layered onto a 10

mL linear sucrose gradient (15–40% w/v) and centrifuged (Beckman SW41Ti) for 2h at 38,000 rpm at 4°C. Fractions were collected and digested with 100 µg proteinase K in 1% SDS and 10 mM EDTA for 30 min at 37°C. RNA was recovered using phenol-chloroform-isomyl alcohol followed by ethanol precipitation.

2.6 RNA Isolation and Analysis

Total RNA was extracted with Trizol reagent using the manufacturer's protocol (Invitrogen, Carlsbad, CA) or as described above. For Real Time PCR, reverse transcription was performed using 0.5 µg of DNase-treated RNA, Superscript II RnaseH- and random hexamers. PCR reactions were performed in 96 well plates using transcribed cDNA and IQ-SYBR green master mix (Bio Rad, Hercules, CA). PCR efficiency was between 90–105% for all primer and probe sets and linear over 5 orders of magnitude. The specificity of products generated for each set of primers was examined for each fragment using a melting curve and gel electrophoresis. Reactions were run in triplicate and data calculated as the change in cycle threshold (CT) for the target gene relative to the CT for β_2 -microglobulin and cyclophilin (control genes) according to the procedures of Muller et al. [22]. Results were similar regardless of the control gene; therefore data in the results section are reported using β_2 -microglobulin. Mouse primer sequences (5'-3') were: *CHOP*: forward CGCTCTCCAGATTCCAGTCAG, reverse GTTCTCCTGCTCCTTCTCCTTC; *GADD34*: forward GAGATTCCTCTAAAAGCTCGG, reverse TCTCTCCTGGTAGACAACGC; *GRP78*: forward GAGGCGTATTTGGGAAAGAAGG, reverse GCTGCTGTAGGCTCATTGATG; *Caspase-1*: forward AGATGGCACATTTCCAGGAC, reverse GATCCTCCAGCAGCAACTTC; *Col1a1*: forward CCGCCGATGTCGCTATCC, reverse TCTTGAGGTTGCCAGTCTGC; *IL-1 α* : forward CACGGGGACTGCCCTCTAT, reverse TGTCGGGGTGGCTCCACT; *IL-1 β* : forward TCTTTGAAGTTGACGGACCC, reverse TGAGTGATACTGCCTGCCTG; *IL-33*: forward AGCTCTCCACCGGGGCTCAC, reverse CCTGCGGTGCTGCTGAACT; *NLRP3*: forward AGCCTTCCAGGATCCTCTTC, reverse CTTGGGCAGCAGTTTCTTTC; *SREBP-1c*: forward TGGTGGGCACTGAAGCAAAG, reverse CACTTCGTAGGGTCAGGTTCTC; *α SMA*: forward GCACCACTGAACCCTAAGG, reverse CCAGAGTCCAGCACAATACC; *TGF β 1*: forward TGGACACACAGTACAGCAAGG, reverse GTAGTAGACGATGGGCAGTGG; *XBPIs*: forward GTCTGCTGAGTCCGCAGCAGG, reverse GATTAGCAGACTCTGGGGAAG.

2.7 Western Blot Analysis

Western blot analysis was performed as described in detail previously [23, 24]. Membranes were incubated with antibodies against Beclin-1 (Cell Signaling, Danvers, MA, #3495), p62 (Cell Signaling, #5114), α -tubulin or β -actin (Cell Signaling, #3873 or #8457), LC3B (Novus, Littleton, CO, #NB600-1384), AMPK (AMP-activated protein kinase; Cell Signaling, total = #5831; phosphorylated = #4188), eIF-2 α (eukaryotic initiation factor-2 α ; Santa Cruz Biotechnology, Santa Cruz, CA; #sc133132), and phosphorylated eIF-2 α (Abcam; #Ab32157). Proteins were detected with horseradish peroxidase-conjugated secondary antibodies (GE Healthcare Bio-Sciences, Marlborough, MA) and an enhanced chemiluminescence reagent (Pierce, Rockford, IL). Density was quantified using a UVP Bioimaging system (Upland, CA).

2.8 Metabolomic Analysis

Metabolites were extracted from liver tissue, that was flushed of blood prior to removal, with 2:1 chloroform:methanol (v:v) followed by centrifugation ($13000 \times g$, 15 min, 4°C). An internal standard, ^{13}C -glucose, was added to the aqueous extract and the extract was dried. The dried extract was resuspended in methanol, to reduce glycogen, centrifuged and the supernatant dried. This dried extract was resuspended in pyridine containing methoxyamine hydrochloride, incubated at 60°C , sonicated and incubated again at 60°C . N-methyl-N-trimethylsilyltrifluoroacetamide with 1% trimethylchlorosilane was added and the samples were incubated at 60°C . Samples were then centrifuged ($3000 \times g$) for 5 min, cooled to room temperature and a portion transferred to a glass insert in a GC-MS autosampler vial. Metabolites were detected using a Trace GC Ultra coupled to a Thermo ISQ Mass Spectrometer (Thermo Scientific). Samples were injected in a 1:10 split ratio twice in discrete randomized blocks. Separation was achieved using a 30 m TG-5MS column (Thermo Scientific, 0.25 mm i.d., 0.25 μm film thickness) with a 1.2 ml/min helium gas flow rate. The program consisted of 80°C for 30 sec, a ramp of 15°C per min to 330°C , and an 8 min hold. Masses between 50–650 m/z were scanned at 5 scans/sec after electron impact ionization. The ionization source was cleaned and retuned and the injection liner replaced between injection replicates.

2.9 Data Analysis

2.9.1 Metabolomic Analysis—For each sample, molecular features as defined by retention and mass (m/z) were generated using XCMS software in R. Outlier injections were detected based on total signal and PC1 of principle component analysis, and the mean area of the chromatographic peak was calculated among replicate injections. Features were grouped based on a novel clustering tool, RAMClustR, which groups features into spectra based on coelution and covariance across the full experiment. Compounds were annotated based on spectral matching to in-house, NISTv12, Golm, Metlin, and Massbank metabolite databases. The peak areas for each feature in a spectrum were condensed via the weighted mean of all features in a spectrum into a single value for each compound. Analysis of variance was conducted on each compound using the analysis of variance function in R, and p-values were adjusted for false positives using the Bonferroni-Hochberg method in the p.adjust function in R. PCA was conducted on mean-centered and pareto variance-scaled data using the pcaMethods package in R. Trehalose, lactic acid and pyruvic acid were quantified absolutely by external calibration using a 7 point calibration curve with a fixed concentration of ^{13}C labeled glucose as internal standard.

2.9.2 Data presentation and statistics—Results are presented as means \pm standard deviation. Comparisons among groups were determined using ANOVA. Significance was determined using $P < 0.05$.

3. Results

3.1 Glucose and triglycerides

Plasma glucose, plasma triglycerides and liver triglycerides were not significantly different between young and old mice (Fig. 1). Trehalose supplementation did not have a significant

effect on plasma glucose, plasma triglycerides or liver triglycerides in young and old mice (Fig. 1). Food and water intake were not significantly different among groups. Body weight was not significantly different among groups.

3.2 Markers of liver injury

Plasma levels of alanine aminotransferase (ALT) and aspartate aminotransferase (AST) were increased in old compared to young mice (Fig. 2). Trehalose supplementation prevented the increase in both ALT and AST in old mice (Fig. 2A and B). *Colla1* (extracellular matrix component), *TGF β* (marker of fibrosis) and α SMA (marker of fibrosis) mRNA were increased in old compared to young mice (Fig. 2C). In addition, the amount of *Colla1* and *TGF β* mRNA associated with polysomes (marker of increased translation) was increased in old compared to young mice (Fig. 2D). In contrast, *Srebp1c* mRNA associated with polysomes, a transcription factor involved in lipogenesis, was not increased in old compared to young mice (Fig. 2D). Trehalose supplementation prevented the increase in markers of liver injury in old mice (Fig. 2).

3.3 Markers of UPR activation

In mammalian cells, UPR activation typically results from the accumulation of unfolded proteins in the ER lumen or ER stress and involves three ER-localized proteins: double-stranded RNA-dependent protein kinase-like ER kinase (PERK), inositol-requiring 1 α (IRE1 α), and activating transcription factor-6 α (ATF6 α) [25]. PERK activation leads to phosphorylation of the α -subunit of the translation initiation factor eIF2 (p-eIF2 α) and subsequent attenuation of translation initiation. Paradoxically, p-eIF2 α leads to selective translation of mRNAs containing open reading frames, such as activating transcription factor-4 (ATF4) and growth arrest and damage-inducible protein 34 (GADD34). Activation of IRE1 α promotes the splicing of X-box-binding protein-1 (XBP1s) mRNA and subsequent transcription of molecular chaperones (e.g. GRP78) and genes involved in ER-associated degradation (e.g. ER degradation-enhancing α -like protein). Activation of ATF6 α leads to its release from the ER membrane, processing in the Golgi, and entry into the nucleus. Transcriptional targets of ATF6 α include protein chaperones and XBP1. Chronic UPR activation also increases the expression of pro-apoptotic genes/proteins, in particular, CCAAT/enhancer-binding protein homologous protein (Chop).

We examined the UPR at three levels: GRP78, GADD34, Chop gene expression and XBP1 mRNA splicing, phosphorylation of eIF2 α and GRP78 protein expression, and translation of ATF4 and GADD34 via polysome profiling [26, 27]. The expression of Chop, GADD34, and GRP78 mRNA, and the spliced form of XBP1 were increased in old compared to young mice (Fig. 3A). Phosphorylation of eIF2 α (Fig. 3B) and GRP78 protein (Fig. 3C) were increased in old compared to young mice. The amount of GADD34 and ATF4 mRNA associated with polysomes (marker of increased translation) was increased in old compared to young mice (Fig. 3D). Trehalose supplementation prevented the increase in all of these markers of UPR activation (Fig. 3).

3.4 Inflammatory Signaling

Plasma levels of IL1 β were not detectable, a finding consistent with other studies in aging mice [28]. Plasma levels of IL6 and IL18 were significantly increased in old compared to young mice (Fig. 4A). Trehalose supplementation prevented the increase in plasma IL6 and IL18 in old mice (Fig. 4A). Liver inflammatory signaling was monitored using the phosphorylation of c-Jun terminal kinase or JNK [7, 29]. Phosphorylation of JNK was increased in old compared to young mice (Fig. 4B). Trehalose supplementation prevented the increase in phosphorylation of JNK in old mice (Fig. 4B). Inflammasomes are caspase-1 activating multi-protein complexes that sense both exogenous and endogenous danger signals through intracellular NOD-like receptors (NLRs) [30]. Activation of inflammasomes involves a priming step, that involves upregulation of genes encoding proteins that make up the multi-protein complex, and an activation step, that involves activation of caspase-1 [30]. Activation of the NLRP3 inflammasome has not only been linked to functional decline in aging but can also be induced by the ER UPR [8, 28, 31]. Therefore, we measured priming and activation of NLRP3 in the livers of old and young mice. IL-1 β , IL1-33 and caspase-1 mRNA and caspase-1 activity were increased in old compared to young mice (Fig. 4C and D). Trehalose supplementation prevented these increases in old mice (Fig. 4C and D).

3.5 Liver metabolites

Trehalose supplementation resulted in a 2.5 fold increase in liver trehalose concentrations in young and old mice (Fig. 5A). The glycolytic metabolites, pyruvate and lactate, were significantly reduced in the liver of old compared to young mice (Fig. 5B and C). Trehalose supplementation prevented these changes in old mice (Fig. 5B and C).

Nicotinamide (NAM) has been linked to neuronal cell survival during anoxic stress and protection against high glucose/palmitate-induced β -cell toxicity [32, 33]. Genetic or pharmacologic approaches that increase the hexosamine biosynthetic pathway metabolite, UDP-N-acetylglucosamine, extended longevity and ameliorated disruptions in proteostasis in *C. elegans* [34]. In the present study, liver NAM and UDP-N-acetylhexosamines (UDP-N-acetylglucosamine + UDP-N-acetylgalactosamine) were reduced in the liver of old compared to young mice (Fig. 5D and E). Trehalose supplementation prevented these changes (Fig. 5D and E).

3.6 Markers of protein degradative capacity and autophagy

Beclin-1, a member of the lipid-kinase complex involved in initiation and regulation of macroautophagy [35], was reduced in the liver of old compared to young mice (Fig. 6A). A protein marker of undegraded autophagy substrates [35], p62, was increased in the liver of old compared to young mice (Fig. 6B). Trehalose supplementation prevented these changes in old mice (Fig. 6A and B). The ratio of LC3B-II to α -tubulin and phosphorylation of AMPK were increased in old mice treated with trehalose (Fig. 6C and D). Proteasome activity in the liver was reduced in old compared to young mice (Fig. 6E). Trehalose supplementation restored proteasome activity in old mice to values observed in young mice (Fig. 6E).

4. Discussion

Impairments in proteostasis and recruitment of inflammatory pathways have been identified as hallmark characteristics of aging in a number of model organisms and mammalian tissues, including the liver [5, 13, 36, 37]. Recent studies have demonstrated that the aging liver is characterized by changes in metabolism that can contribute to hepatic steatosis, activation of inflammatory signaling pathways, impaired protein stability and activation of protein quality control pathways such as the ER UPR [28, 30, 38–41]. Trehalose, a non-reducing disaccharide, is synthesized in response to cellular stressors such as heat, cold, and desiccation in a number of organisms [1]. In mammalian systems, trehalose has proven effective in reducing impairments in proteostasis via mechanisms that include increased protein stability and activation of protein clearance pathways [2, 3]. In the present study, we examined the ability of trehalose to reduce or prevent age-associated activation of the ER UPR and inflammatory signaling, as well as markers of liver injury. The results of this study demonstrate that trehalose supplementation reduced activation of the ER UPR, inflammatory signaling and liver injury in old mice.

The ER UPR represents a network of signaling pathways that respond to stress in the ER (i.e. accumulation of unfolded proteins in the ER lumen). The general output of the ER UPR is upregulation of genes involved in ER protein folding and degradation, attenuation of general translation and selective translation of genes such as ATF4 and GADD34 [42, 43]. In the present study, we monitored the ER UPR at the gene, protein and translational level. Our data demonstrate that the ER UPR was activated in the liver of old mice, suggesting that the ER in aging mice is characterized by the accumulation of unfolded proteins or ER stress. These data are consistent with the concept that impairments of proteostasis contribute to or result from the aging process [5, 36]. Trehalose supplementation over a 4 wk period mitigated the activation of the ER UPR in the liver of old mice. Therefore, this study has identified trehalose as an effective treatment against aging-induced activation of the ER UPR in the liver.

Low grade inflammation is a common feature of age-related co-morbidities such as cardiovascular disease, insulin resistance, metabolic syndrome and type 2 diabetes [7, 44]. Inflammation has also been linked to neurological disorders associated with aging and to the aging process in general [45, 46]. In the present study, we monitored both liver and systemic inflammatory signaling in young and old mice. Our data demonstrate that liver inflammatory signaling was increased (i.e. increased phosphorylation of JNK, increased inflammasome gene expression, increased caspase-1 activity) in old mice [28, 29]. In addition, old mice were characterized by increased plasma levels of IL6 and IL18, consistent with a systemic inflammatory response [28]. Trehalose supplementation over a 4 wk period prevented the increase in both liver and systemic inflammatory signaling in old mice. Chronic activation of the ER UPR has been linked to the activation of inflammatory signaling involving JNK and the inflammasome [8, 47]. Increased inflammatory signaling can also activate the ER UPR [48]. Although the present study cannot identify the primary target of trehalose, it does demonstrate that trehalose effectively reduced both ER UPR activation and inflammatory signaling in old mice. Perhaps most importantly, trehalose prevented the increase in multiple indices (Fig. 2) of liver injury in old mice.

Previous studies have demonstrated that trehalose can stabilize proteins and activate autophagy [1–4]. The most recent of these studies provided convincing evidence that trehalose-mediated activation of autophagy involved inhibition of the solute carrier 2A family of glucose transporters and activation of adenosine 5'-monophosphate-activated protein kinase (AMPK)-dependent autophagy [4]. In the present study, we monitored proteins involved in autophagy and phosphorylation of AMPK, as well as, proteasome activity in order to better understand how aging and trehalose influence systems involved in protein and damaged organelle clearance. In the present study, old mice were characterized by reduced expression of Beclin-1 and increased expression of p62, changes associated with reduced autophagic capacity [35]. In addition, proteasome activity was reduced in the liver of old compared to young mice. These data are consistent with the notion that the capacity for protein clearance was reduced in the liver of old mice. Trehalose supplementation restored Beclin-1, p62 and proteasome activity to levels observed in young mice. Trehalose supplementation also increased phosphorylation of AMPK and LC3B-II in old mice. It is important to note that the approach used to assess LC3B-II in the present study only assessed the accumulation of this protein and not autophagic flux [49]. Nonetheless, the data in total suggests that trehalose improved the capacity for protein clearance in the liver of old mice. We hypothesize that trehalose-mediated improvements in protein clearance reduce the need for ER UPR activation and the resultant engagement of inflammatory signaling.

Although recent work by DeBosch and colleagues suggests that trehalose-mediated activation of autophagy involves inhibition of glucose transport [4], there is very little information on the metabolite profile in the liver following in the liver following trehalose exposure. In the present study, metabolite analyses demonstrated that trehalose supplementation increased liver trehalose concentrations to a similar extent in both young and old mice. This observation suggests that trehalose per se may not mediate the beneficial effects observed in old mice (e.g. prevention of the activation of the ER UPR in the liver of old mice), given that the liver of young mice was not characterized by increased phosphorylation of AMPK or accumulation of LC3B-II. The glycolytic metabolites, pyruvate and lactate, were reduced in old compared to young mice and trehalose treatment resulted in normalization of pyruvate and lactate concentrations in the liver of old mice. These novel results suggest that trehalose, through unknown mechanism, can influence steady state concentrations of pyruvate and lactate in old mice. It should also be noted that the presence of low levels of trehalose in the liver of control mice suggests that there are low levels of trehalose in the chow diet (as we could not detect trehalose in regular drinking water). NAM and UDP-N-acetylhexosamine concentrations were reduced in old compared to young mice and trehalose treatment resulted in their normalization. It is interesting that NAM can promote the extension of replicative lifespan of human cells but can also serve as an inhibitor of sirtuins (energy-sensing enzymes that may mediate lifespan) [32, 50]. Given that NAM depletion can activate Sirtuin 2 and promote lifespan, data from the present study suggest that any beneficial effect of NAM on hepatic function is likely sirtuin independent [51]. The hexosamine biosynthetic pathway converts fructose-6-phosphate to UDP-N-acetylglucosamine and UDP-N-acetylgalactosamine to support N- and O-linked glycosylation. In *C. elegans* increased UDP-Hex extended lifespan and improved protein quality control via mechanisms that included increased autophagy, ER-associated

degradation and proteasome activity [34]. Therefore, the ability of trehalose to influence the ER UPR, autophagy and proteasome activity may also involve its ability to maintain hexosamine pathway metabolites. Additional studies are necessary to examine this possibility.

There are limitations to the present study that should be acknowledged. In the present study, old mice were at ~50% survival age and therefore were at a very late stage of the lifespan. Future studies will be needed to examine links between trehalose, ER proteostasis and inflammatory signaling in the liver throughout the lifespan. We did not evaluate hepatic inflammation histologically in the present study. Therefore, we do not know the extent of hepatic inflammation in the liver of old mice nor whether trehalose can modulate this inflammation. One of the main outcomes of NLRP3 inflammasome activation is the production of IL-1 β . In the present study we were unable to detect IL-1 β in the plasma of old and young mice. This result is consistent with other studies that have examined aging and the NLRP3 inflammasome in the absence of an exogenous inflammatory stimulus [28].

In summary, this study demonstrated that the liver of old mice was characterized by activation of the ER UPR and inflammatory signaling, reduced nicotinamide and UDP-N-acetyl-hexosamines, and reduced proteasome activity. Trehalose restored all of these changes to levels observed in young mice. Trehalose also increased the phosphorylation of AMPK and accumulation of LC3B-II in the liver of old mice. Therefore, trehalose appears to be an effective therapeutic strategy to counteract age-associated impairments in proteostasis in the liver.

Acknowledgments

Funding Sources: This work was supported by NIH grant DK072017 and the Lillian Fountain Smith Endowment (MJP), NIH MERIT award AG013038 (DRS), and a pre-doctoral NRSA Fellowship, AG0039210 (TJL). Key Words: Aging, inflammation, unfolded protein response, liver, hexosamine biosynthetic pathway, proteostasis

The authors thank the Proteomics and Metabolomics Facility at Colorado State University for metabolomics and bioinformatics analyses.

References

1. Jain NK, Roy I. Effect of trehalose on protein structure. *Protein Sci.* 2009; 18:24–36. [PubMed: 19177348]
2. Tanaka M, Machida Y, Niu S, Ikeda T, Jana NR, Doi H, Kurosawa M, Nekooki M, Nukina N. Trehalose alleviates polyglutamine-mediated pathology in a mouse model of Huntington disease. *Nat Med.* 2004; 10:148–154. [PubMed: 14730359]
3. Rodriguez-Navarro JA, Rodriguez L, Casarejos MJ, Solano RM, Gomez A, Perucho J, Cuervo AM, Garcia de Yebenes J, Mena MA. Trehalose ameliorates dopaminergic and tau pathology in parkin deleted/tau overexpressing mice through autophagy activation. *Neurobiol Dis.* 2010; 39:423–438. [PubMed: 20546895]
4. DeBosch BJ, Heitmeier MR, Mayer AL, Higgins CB, Crowley JR, Kraft TE, Chi M, Newberry EP, Chen Z, Finck BN, et al. Trehalose inhibits solute carrier 2A (SLC2A) proteins to induce autophagy and prevent hepatic steatosis. *Sci Signal.* 2016; 9:ra21. [PubMed: 26905426]
5. Ben-Zvi A, Miller EA, Morimoto RI. Collapse of proteostasis represents an early molecular event in *Caenorhabditis elegans* aging. *Proc Natl Acad Sci U S A.* 2009; 106:14914–14919. [PubMed: 19706382]

6. Taylor RC, Dillin A. Aging as an event of proteostasis collapse. *Cold Spring Harb Perspect Biol.* 2011; 3
7. Hotamisligil GS. Endoplasmic reticulum stress and the inflammatory basis of metabolic disease. *Cell.* 2010; 140:900–917. [PubMed: 20303879]
8. Lerner AG, Upton JP, Praveen PV, Ghosh R, Nakagawa Y, Igarria A, Shen S, Nguyen V, Backes BJ, Heiman M, et al. IRE1 α induces thioredoxin-interacting protein to activate the NLRP3 inflammasome and promote programmed cell death under irremediable ER stress. *Cell Metab.* 2012; 16:250–264. [PubMed: 22883233]
9. Zhang K, Kaufman RJ. From endoplasmic-reticulum stress to the inflammatory response. *Nature.* 2008; 454:455–462. [PubMed: 18650916]
10. Le Couteur DG, Cogger VC, Markus AM, Harvey PJ, Yin ZL, Anselin AD, McLean AJ. Pseudocapillarization and associated energy limitation in the aged rat liver. *Hepatology.* 2001; 33:537–543. [PubMed: 11230732]
11. Hilmer SN, Cogger VC, Le Couteur DG. Basal activity of Kupffer cells increases with old age. *J Gerontol A Biol Sci Med Sci.* 2007; 62:973–978. [PubMed: 17895435]
12. Naidoo N. ER and aging-Protein folding and the ER stress response. *Ageing Res Rev.* 2009; 8:150–159. [PubMed: 19491040]
13. Park JH, Chung HY, Kim M, Lee JH, Jung M, Ha H. Daumone fed late in life improves survival and reduces hepatic inflammation and fibrosis in mice. *Ageing Cell.* 2014; 13:709–718. [PubMed: 24796965]
14. Zhang C, Cuervo AM. Restoration of chaperone-mediated autophagy in aging liver improves cellular maintenance and hepatic function. *Nat Med.* 2008; 14:959–965. [PubMed: 18690243]
15. Elsliger MA, Dallaire L, Potier M. Fetal intestinal and renal origins of trehalase activity in human amniotic fluid. *Clin Chim Acta.* 1993; 216:91–102. [PubMed: 8222277]
16. Eze LC. Plasma trehalase activity and diabetes mellitus. *Biochem Genet.* 1989; 27:487–495. [PubMed: 2619709]
17. Murray IA, Coupland K, Smith JA, Ansell ID, Long RG. Intestinal trehalase activity in a UK population: establishing a normal range and the effect of disease. *Br J Nutr.* 2000; 83:241–245. [PubMed: 10884712]
18. LaRocca TJ, Henson GD, Thorburn A, Sindler AL, Pierce GL, Seals DR. Translational evidence that impaired autophagy contributes to arterial ageing. *J Physiol.* 2012; 590:3305–3316. [PubMed: 22570377]
19. Vanhooren V, Libert C. The mouse as a model organism in aging research: usefulness, pitfalls and possibilities. *Ageing Res Rev.* 2013; 12:8–21. [PubMed: 22543101]
20. Bligh EG, Dyer WJ. A rapid method of total lipid extraction and purification. *Can J Biochem Physiol.* 1959; 37:911–917. [PubMed: 13671378]
21. del Prete MJ, Vernal R, Dolznig H, Mullner EW, Garcia-Sanz JA. Isolation of polysome-bound mRNA from solid tissues amenable for RT-PCR and profiling experiments. *RNA.* 2007; 13:414–421. [PubMed: 17237355]
22. Muller PY, Janovjak H, Miserez AR, Dobbie Z. Processing of gene expression data generated by quantitative real-time RT-PCR. *Biotechniques.* 2002; 32:1372–1374. 1376, 1378–1379. [PubMed: 12074169]
23. Pagliassotti MJ, Kang J, Thresher JS, Sung CK, Bizeau ME. Elevated basal PI 3-kinase activity and reduced insulin signaling in sucrose-induced hepatic insulin resistance. *Am J Physiol Endocrinol Metab.* 2002; 282:E170–176. [PubMed: 11739098]
24. Wei Y, Wang D, Topczewski F, Pagliassotti MJ. Saturated fatty acids induce endoplasmic reticulum stress and apoptosis independently of ceramide in liver cells. *Am J Physiol Endocrinol Metab.* 2006; 291:E275–E281. [PubMed: 16492686]
25. Rutkowski DT, Kaufman RJ. A trip to the ER: coping with stress. *Trends Cell Biol.* 2004; 14:20–28. [PubMed: 14729177]
26. Hatanaka M, Maier B, Sims EK, Templin AT, Kulkarni RN, Evans-Molina C, Mirmira RG. Palmitate induces mRNA translation and increases ER protein load in islet beta-cells via activation of the mammalian target of rapamycin pathway. *Diabetes.* 2014; 63:3404–3415. [PubMed: 24834975]

27. Fu S, Fan J, Blanco J, Gimenez-Cassina A, Danial NN, Watkins SM, Hotamisligil GS. Polysome profiling in liver identifies dynamic regulation of endoplasmic reticulum translome by obesity and fasting. *PLoS Genet.* 2012; 8:e1002902. [PubMed: 22927828]
28. Youm YH, Grant RW, McCabe LR, Albarado DC, Nguyen KY, Ravussin A, Pistell P, Newman S, Carter R, Laque A, et al. Canonical Nlrp3 inflammasome links systemic low-grade inflammation to functional decline in aging. *Cell Metab.* 2013; 18:519–532. [PubMed: 24093676]
29. Hirosumi J, Tuncman G, Chang L, Gorgun CZ, Uysal KT, Maeda K, Karin M, Hotamisligil GS. A central role for JNK in obesity and insulin resistance. *Nature.* 2002; 420:333–336. [PubMed: 12447443]
30. Szabo G, Csak T. Inflammasomes in liver diseases. *J Hepatol.* 2012; 57:642–654. [PubMed: 22634126]
31. Menu P, Mayor A, Zhou R, Tardivel A, Ichijo H, Mori K, Tschopp J. ER stress activates the NLRP3 inflammasome via an UPR-independent pathway. *Cell Death Dis.* 2012; 3:e261. [PubMed: 22278288]
32. Chong ZZ, Lin SH, Li F, Maiese K. The sirtuin inhibitor nicotinamide enhances neuronal cell survival during acute anoxic injury through AKT, BAD, PARP, and mitochondrial associated “anti-apoptotic” pathways. *Curr Neurovasc Res.* 2005; 2:271–285. [PubMed: 16181120]
33. Lee SJ, Choi SE, Jung IR, Lee KW, Kang Y. Protective effect of nicotinamide on high glucose/palmitate-induced glucolipotoxicity to INS-1 beta cells is attributed to its inhibitory activity to sirtuins. *Arch Biochem Biophys.* 2013; 535:187–196. [PubMed: 23562377]
34. Denzel MS, Storm NJ, Gutschmidt A, Baddi R, Hinze Y, Jarosch E, Sommer T, Hoppe T, Antebi A. Hexosamine pathway metabolites enhance protein quality control and prolong life. *Cell.* 2014; 156:1167–1178. [PubMed: 24630720]
35. Tucci M, Stucci S, Savonarola A, Resta L, Cives M, Rossi R, Silvestris F. An imbalance between Beclin-1 and p62 expression promotes the proliferation of myeloma cells through autophagy regulation. *Exp Hematol.* 2014; 42:897–908. e891. [PubMed: 24971696]
36. Dubnikov T, Cohen E. Proteostasis collapse, inter-tissue communication, and the regulation of aging at the organismal level. *Front Genet.* 2015; 6:80. [PubMed: 25798145]
37. Lopez-Otin C, Blasco MA, Partridge L, Serrano M, Kroemer G. The hallmarks of aging. *Cell.* 2013; 153:1194–1217. [PubMed: 23746838]
38. Kuhla A, Blei T, Jaster R, Vollmar B. Aging is associated with a shift of fatty metabolism toward lipogenesis. *J Gerontol A Biol Sci Med Sci.* 2011; 66:1192–1200. [PubMed: 21835806]
39. Decuypere JP, Monaco G, Missiaen L, De Smedt H, Parys JB, Bultynck G. IP(3) Receptors, Mitochondria, and Ca Signaling: Implications for Aging. *J Aging Res.* 2011; 2011:920178. [PubMed: 21423550]
40. Perez VI, Buffenstein R, Masamsetti V, Leonard S, Salmon AB, Mele J, Andziak B, Yang T, Edrey Y, Friguet B, et al. Protein stability and resistance to oxidative stress are determinants of longevity in the longest-living rodent, the naked mole-rat. *Proc Natl Acad Sci U S A.* 2009; 106:3059–3064. [PubMed: 19223593]
41. Xiong X, Wang X, Lu Y, Wang E, Zhang Z, Yang J, Zhang H, Li X. Hepatic steatosis exacerbated by endoplasmic reticulum stress-mediated downregulation of FXR in aging mice. *J Hepatol.* 2014; 60:847–854. [PubMed: 24333182]
42. Kaufman RJ. Stress signaling from the lumen of the endoplasmic reticulum: coordination of gene transcriptional and translational controls. *Genes Dev.* 1999; 13:1211–1233. [PubMed: 10346810]
43. Rutkowski DT, Hegde RS. Regulation of basal cellular physiology by the homeostatic unfolded protein response. *J Cell Biol.* 2010; 189:783–794. [PubMed: 20513765]
44. de Gonzalo-Calvo D, Neitzert K, Fernandez M, Vega-Naredo I, Caballero B, Garcia-Macia M, Suarez FM, Rodriguez-Colunga MJ, Solano JJ, Coto-Montes A. Differential inflammatory responses in aging and disease: TNF-alpha and IL-6 as possible biomarkers. *Free Radic Biol Med.* 2010; 49:733–737. [PubMed: 20639132]
45. Heneka MT, Carson MJ, El Khoury J, Landreth GE, Brosseron F, Feinstein DL, Jacobs AH, Wyss-Coray T, Vitorica J, Ransohoff RM, et al. Neuroinflammation in Alzheimer’s disease. *Lancet Neurol.* 2015; 14:388–405. [PubMed: 25792098]

46. Marchalant Y, Brothers HM, Wenk GL. Inflammation and aging: can endocannabinoids help? *Biomed Pharmacother.* 2008; 62:212–217. [PubMed: 18400455]
47. Ozcan U, Cao Q, Yilmaz E, Lee AH, Iwakoshi NN, Ozdelen E, Tuncman G, Gorgun C, Glimcher LH, Hotamisligil GS. Endoplasmic reticulum stress links obesity, insulin action, and type 2 diabetes. *Science.* 2004; 306:457–461. [PubMed: 15486293]
48. Xue X, Piao JH, Nakajima A, Sakon-Komazawa S, Kojima Y, Mori K, Yagita H, Okumura K, Harding H, Nakano H. Tumor necrosis factor alpha (TNFalpha) induces the unfolded protein response (UPR) in a reactive oxygen species (ROS)-dependent fashion, and the UPR counteracts ROS accumulation by TNFalpha. *J Biol Chem.* 2005; 280:33917–33925. [PubMed: 16107336]
49. Klionsky DJ, Abdalla FC, Abeliovich H, Abraham RT, Acevedo-Arozena A, Adeli K, Agholme L, Agnello M, Agostinis P, Aguirre-Ghiso JA, et al. Guidelines for the use and interpretation of assays for monitoring autophagy. *Autophagy.* 2012; 8:445–544. [PubMed: 22966490]
50. Kang HT, Lee HI, Hwang ES. Nicotinamide extends replicative lifespan of human cells. *Aging Cell.* 2006; 5:423–436. [PubMed: 16939485]
51. Anderson RM, Bitterman KJ, Wood JG, Medvedik O, Sinclair DA. Nicotinamide and PNC1 govern lifespan extension by calorie restriction in *Saccharomyces cerevisiae*. *Nature.* 2003; 423:181–185. [PubMed: 12736687]

Highlights

1. The liver of old mice is characterized by endoplasmic reticulum stress, increased inflammatory signaling, liver injury and reduced proteasome activity.
2. Trehalose treatment over a 4 wk period reduced endoplasmic reticulum stress, inflammatory signaling, liver injury and restored proteasome activity.
3. Trehalose treatment increased markers of autophagy.
4. Trehalose results in restoration of glycolytic metabolites and hexosamine biosynthetic pathway metabolites in the liver of old mice.

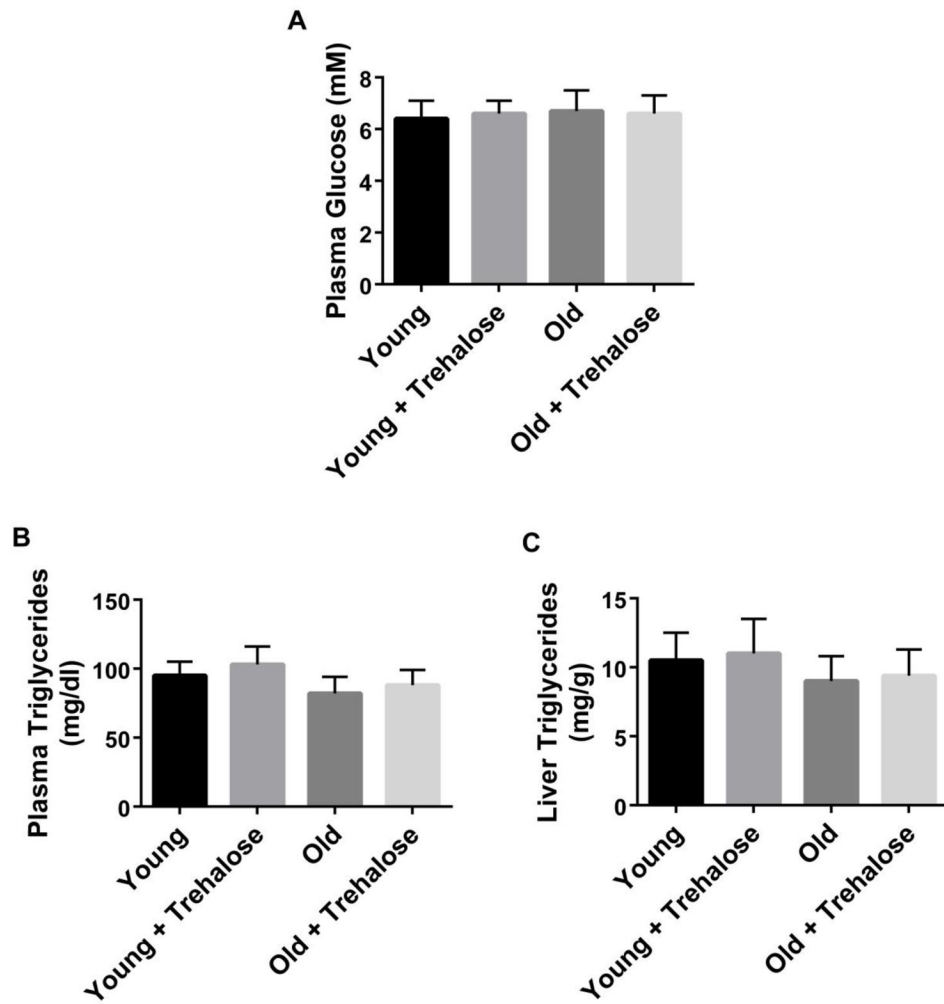


Figure 1. Plasma and liver metabolites. A, Plasma glucose; B, Plasma triglycerides; C, Liver triglycerides in young and old mice in the absence or presence trehalose in the drinking water (+ trehalose: 2% trehalose for 4 weeks). Values are means \pm SDEV for $n=7-8$ per group.

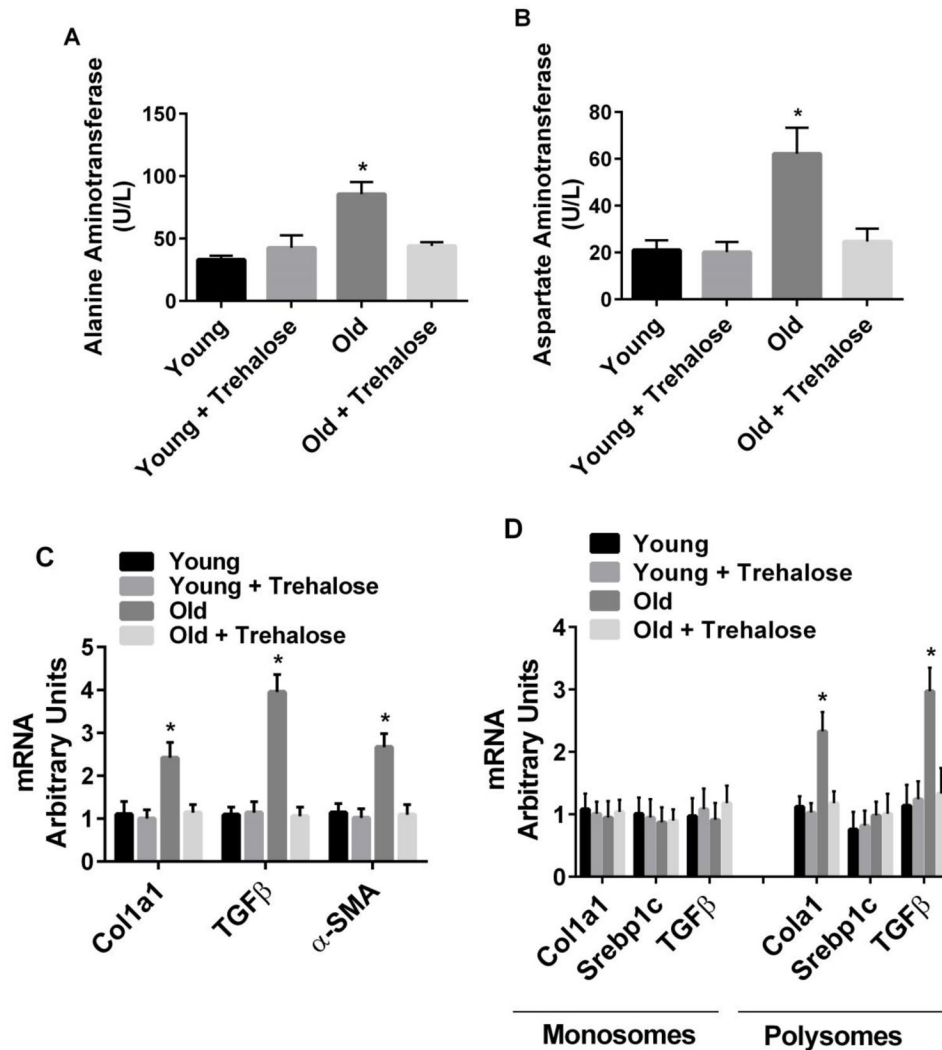


Figure 2. Markers of liver injury. A, Alanine aminotransferase; B, Aspartate aminotransferase; C, Gene markers of cell matrix and fibrosis; D, Translation of genes involved in matrix formation and fibrosis in young and old mice in the absence or presence trehalose in the drinking water (+ trehalose: 2% trehalose for 4 weeks). Srebp1c, a transcription factor involved in lipogenesis, was used as a negative control in monosome and polysome assays. Values are means \pm SDEV for n=7–8 per group. * P<0.05 vs. other groups.

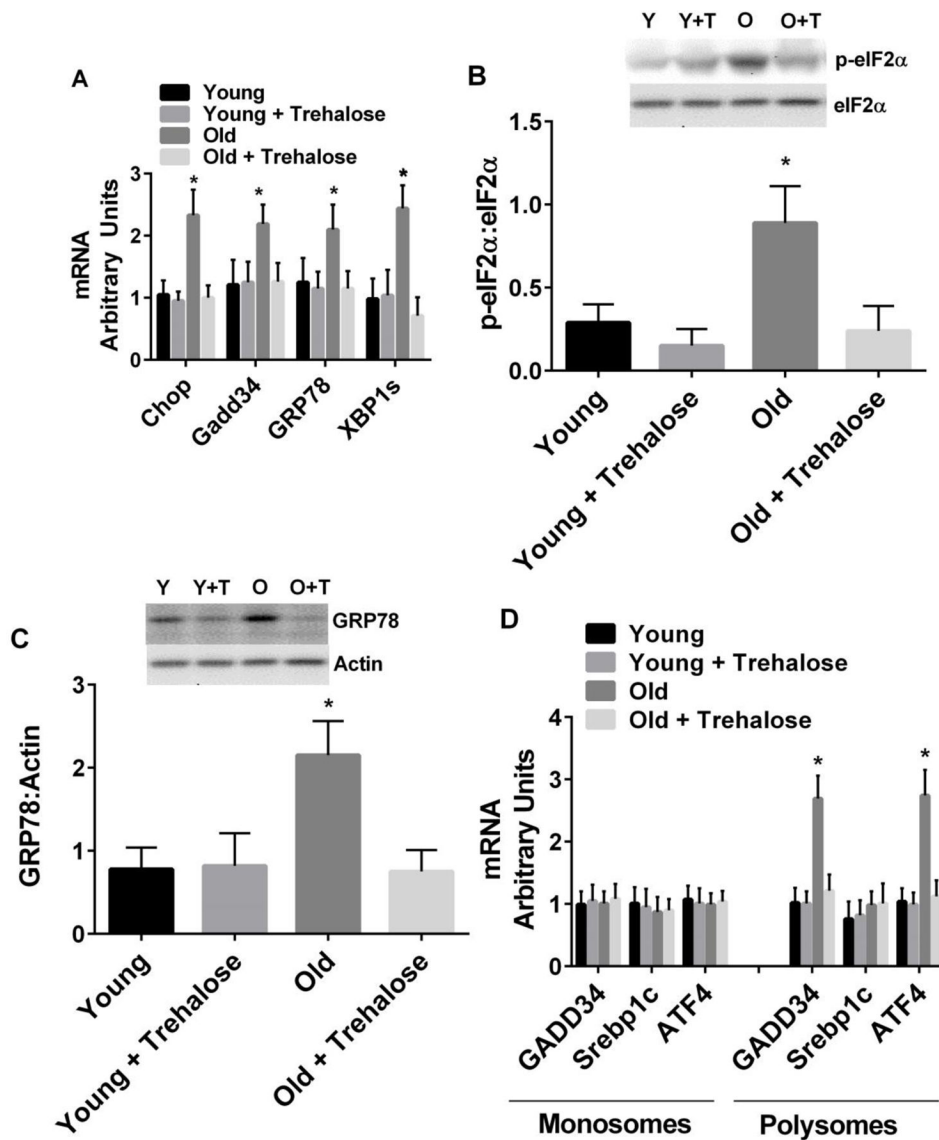


Figure 3. Markers of the ER-UPR. A, Liver gene expression and XBP1 mRNA splicing; B, Phosphorylation of eIF2 α ; C, GRP78 protein expression; D, Translation of GADD34 and ATF4 mRNA in young and old mice in the absence or presence trehalose in the drinking water (+ trehalose: 2% trehalose for 4 weeks). Srebp1c, a transcription factor involved in lipogenesis, was used as a negative control in monosome and polysome assays. Values are means \pm SDEV for n=7–8 per group. Representative gels provided above relevant figures (Y = young, Y+T = young + trehalose, O = old, O+T = old + trehalose). * P<0.05 vs. other groups.

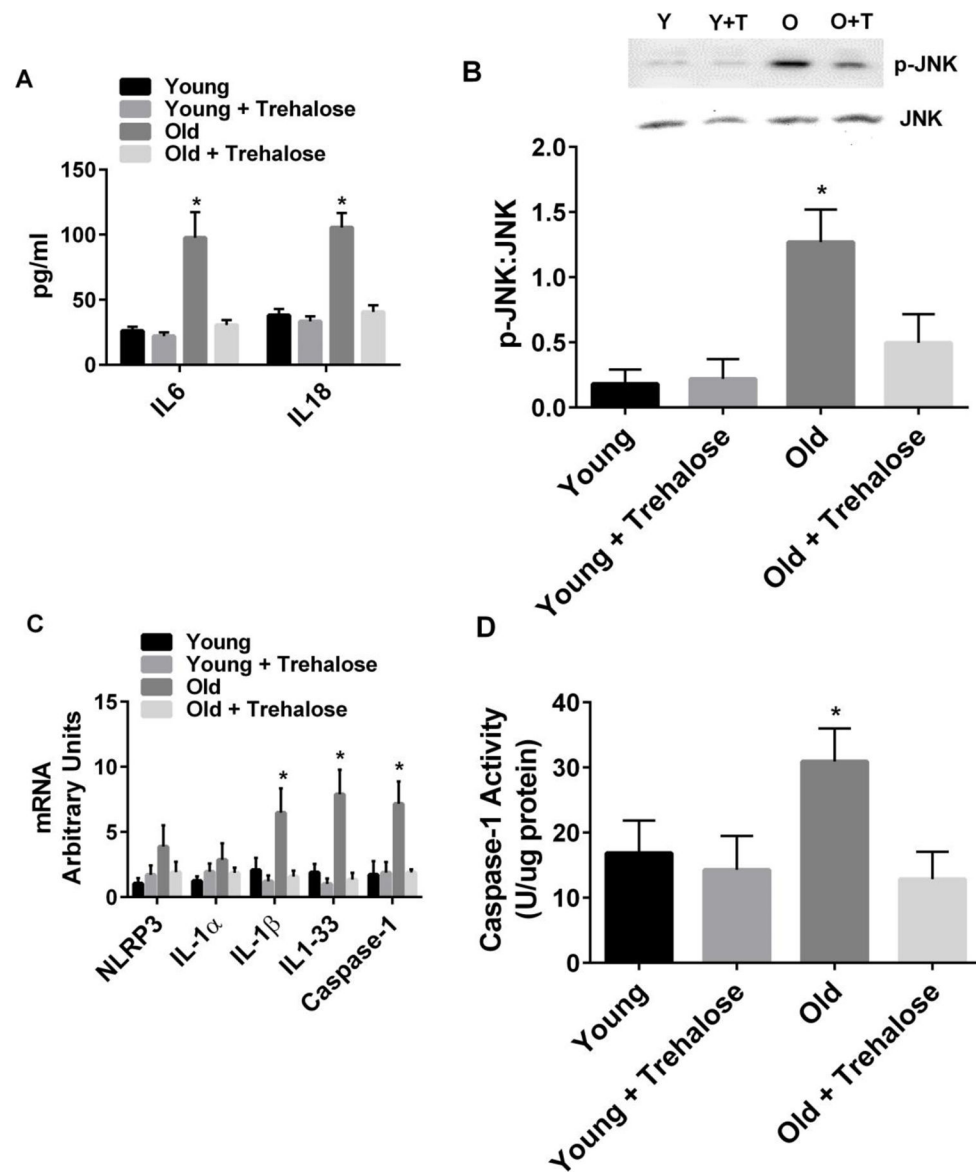


Figure 4.

Markers of inflammatory signaling. A, Plasma IL6 and IL18; B, Phosphorylation of JNK in the liver; C, Inflammasome gene expression; D, Caspase-1 activity in young and old mice in the absence or presence trehalose in the drinking water (+ trehalose: 2% trehalose for 4 weeks). Values are means \pm SDEV for n=7–8 per group. Representative gels provided above relevant figures (Y = young, Y+T = young + trehalose, O = old, O+T = old + trehalose). * P<0.05 vs. other groups.

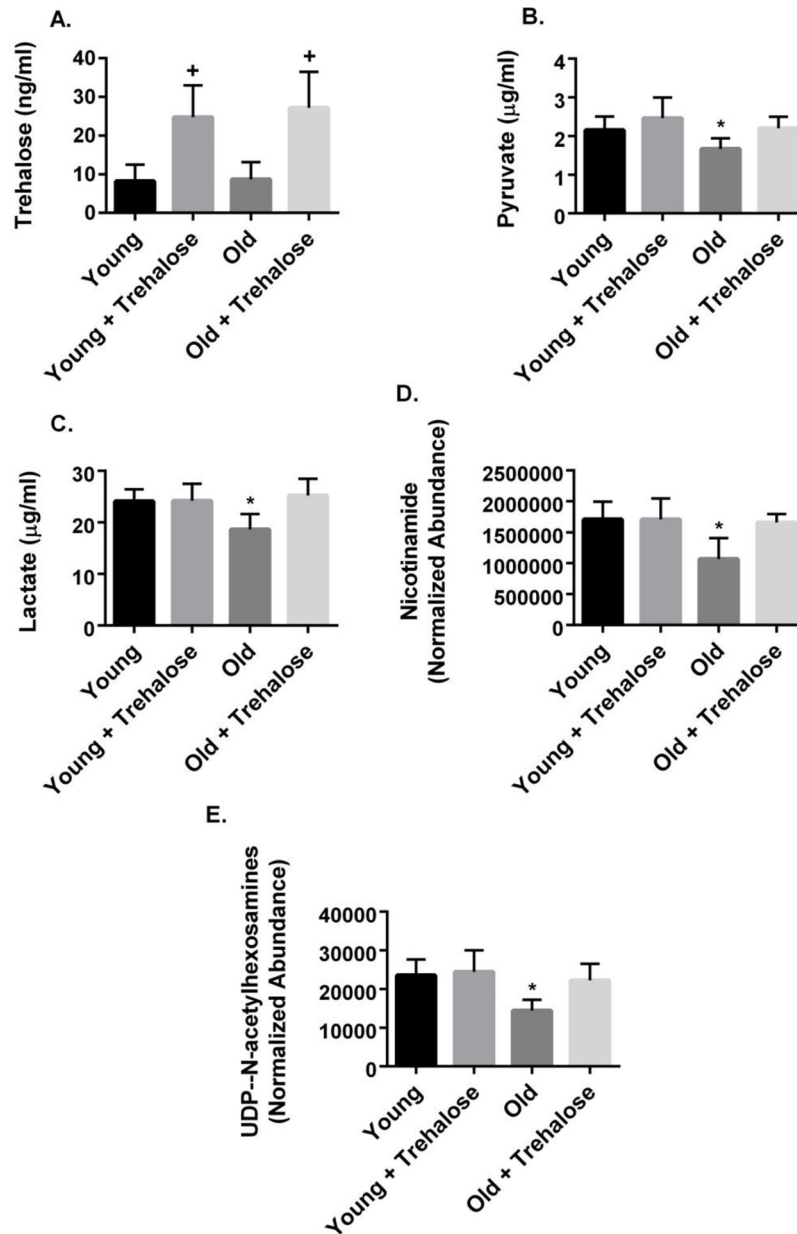


Figure 5. Liver metabolomics. A, Trehalose; B, Pyruvate; C, Lactate; D, Nicotinamide; E, UDP-N-acetylhexosamines (UDP-N-acetylglucosamine + UDP-N-acetylgalactosamine) in young and old mice in the absence or presence trehalose in the drinking water (+ trehalose: 2% trehalose for 4 weeks). Values are means \pm SDEV for $n=7-8$ per group. ⁺, $P<0.05$ vs. young; old; ^{*} $P<0.05$ vs. other groups.

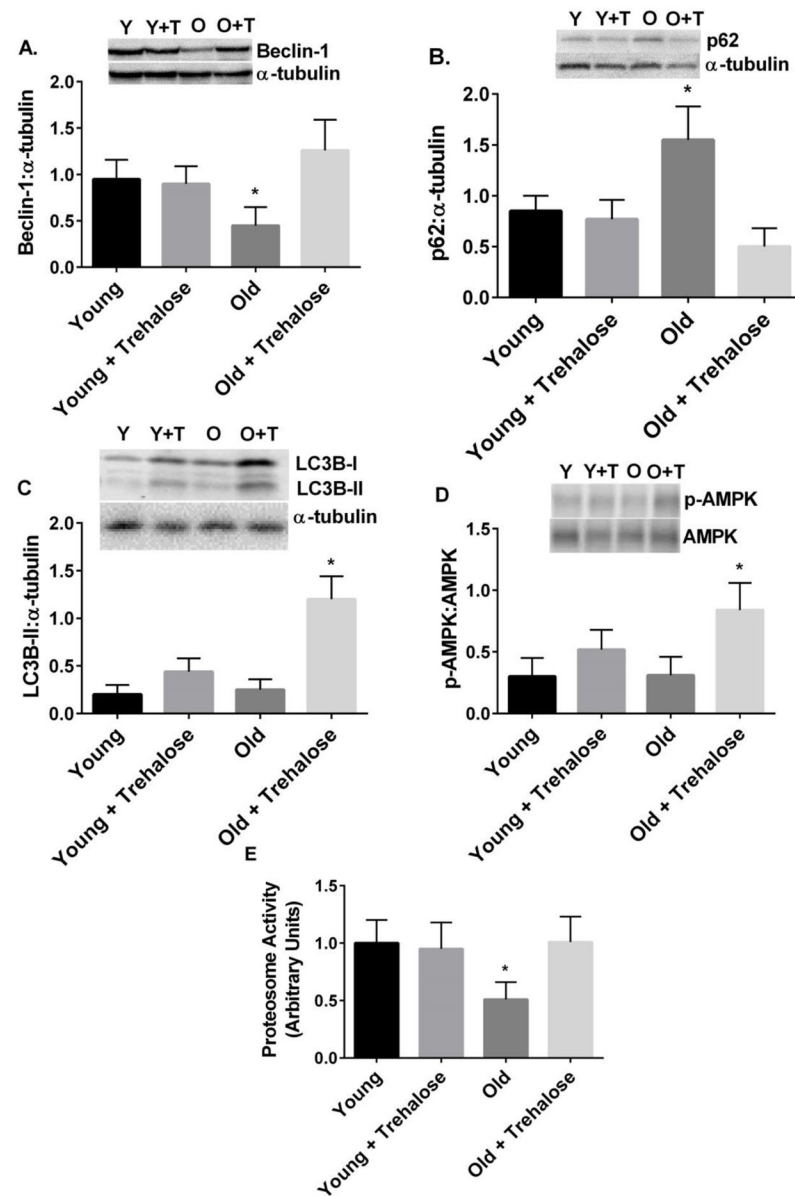


Figure 6. Markers of autophagy and proteasome activity. A, Beclin-1 protein; B, p62 protein; C, LC3BI and II protein; D, Phosphorylation of AMPK; E, Proteasome activity in young and old mice in the absence or presence trehalose in the drinking water (+ trehalose: 2% trehalose for 4 weeks). Values are means \pm SDEV for n=7–8 per group. Representative gels provided above relevant figures (Y = young, Y+T = young + trehalose, O = old, O+T = old + trehalose). * P<0.05 vs. other groups.